Reducing the Satellite Contribution to Range Error

John J. Degnan

Sigma Space Corporation, 4600 Forbes Blvd., Lanham, MD 20706 USA

John.degnan@sigmaspace.com

1. INTRODUCTION

Geodetic satellites (e.g., LAGEOS, Starlette, etc.) are typically in low to medium altitude orbits, have large velocity aberrations, rotate freely in space, and are therefore spherical in shape to permit simultaneous and unbiased ranging from multiple SLR stations. The satellite must present a high enough cross-section, consistent with its altitude, to support ranging by the entire ILRS network. Since velocity aberration limits the size of the individual retroreflectors, cross-section must be achieved by increasing the number of retroreflectors contributing to the station return. Furthermore, the strength of an individual retro return diminishes as one gets farther from normal incidence. To simultaneously achieve maximum range accuracy, the satellite impulse response must be made as short as possible, but the large number of retros, combined with the spherical shape of the surface, causes a variable range between the participating retros and the station, thereby spreading the pulse.

GNSS and Geosynchronous Satellites, on the other hand, have quite different characteristics, i.e.

- Their high orbital altitudes correspond to several Earth radii
- They generally perform a separate utilitarian function (e.g., Earth observation, communications, navigation, etc.) which keeps the nadir side of the satellite approximately facing the Earth CoM. For this reason, flat arrays consisting of many retroreflectors have been used.
- The velocity aberration α is typically between 20 to 25 μrad and the variation is very small [1].

For a typical maximum zenith tracking angle of 70^{o}, beam incidence angles can vary from 0 to θ_{lim} where

$$\theta_{\lim} = a\sin\left[\frac{R_E}{R_E + h}\sin(110^0)\right] \qquad (1)$$

where $R_E = 6371$ km is the mean volumetric radius of the Earth and θ_{lim} equals 13.1^o for GNSS satellites at nominal altitudes (h) of 20,000 km and 8.2^o for Geostationary satellites at nominal altitudes of 36,000 km. The smaller range of incidence angles implies limited pulse spreading from a flat array, especially if the array is compact in size and the retros are densely packed together to achieve the necessary cross-section. Nevertheless, the maximum flat panel induced spreading due to zenith tracking angle is still 474 psec and 292 psec per linear foot of array for GNSS and GEO satellites respectively. This corresponds to a worst case single pulse range measurement spread of 7.1 to 4.4 cm per linear foot for GNSS and GEO satellites respectively as opposed to zero spread when the laser beam is at normal incidence to the array. This spreading can increase further if satellite attitude deviations from true nadir further extend the range of laser incidence angles.

In single photon ranging, satellite spreading is convolved with other sources such as laser pulsewidth and receiver impulse response, to create a wider Probability Distribution Function (PDF) in range which increases the integration time required to achieve a mm precision normal point [2]. In multiphoton ranging, the PDF tends to be narrower with the peak range being skewed toward shorter ranges, resulting in a range bias [3]. In this paper, we examine geodetic satellite designs based on densely packed, large diameter spheres. For GNSS and higher satellites, we propose replacing flat arrays with segments of spheres which would reduce the current angularly dependent satellite spreading with a much shorter impulse response common to all viewing angles. In all cases, the integration time required to achieve 1 mm accuracy normal points is greatly reduced.

2. SPHERICAL GEODETIC SATELLITES

2.1 Satellite Impulse Response

A simple analytical model of spherical satellites has been presented by the author in a previous review article [1]. It was shown that the total time spread (0 to 0) introduced by the satellite is given by the equation

$$\Delta t = \frac{2R_s}{c}\left\{1-\cos\theta_{\max}\left[1-\frac{nL}{R_s}\sqrt{1-\frac{1}{n^2}+\left(\frac{\cos\theta_{\max}}{n}\right)^2}\right]\right\} \cong \frac{R_s}{c}\theta_{\max}^2\left[1-\frac{nL}{R_s}\left(1+\frac{1}{n^2}\right)\right] \tag{2}$$

where c is the speed of light, n = 1.455 is the retro index of refraction for fused quartz, L = 1.095 cm is the retro face to vertex distance for a 38 mm diameter retro, R_s =29.8 cm is the LAGEOS satellite radius, and $\theta_{max} = 43^o$ is the maximum incidence angle accepted by the solid quartz retroreflectors used on LAGEOS. The resulting mean impulse response of the LAGEOS satellite is shown in Figure 2a while Figure 2b shows the good agreement between the exact and approximate versions of Eq. (2).

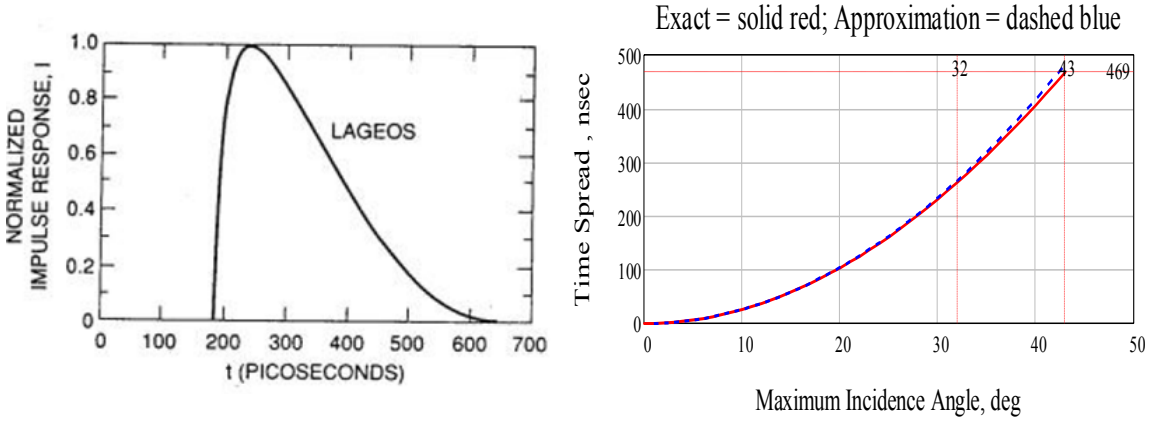

Figure 2: (a) Computed impulse response of the LAGEOS satellite using the model derived in [1];(b) agreement between the exact solution (solid red line) for the total time spread and the approximate solution (dashed blue line) in Eq. (2) is quite good The value of 469 psec for the interval between zeros in the LAGEOS impulse response for a maximum acceptance angle of 43^o agrees with Figure 2a.

2.2 Satellite Optical Cross-Section

In addition to a narrow impulse response, the satellite must also provide adequate optical cross-section for a reasonable probability of detecting the reflected signal. The author's prior model yields the following equation for the peak optical cross-section for a spherical satellite [1]

$$\sigma = \frac{\sigma_{cc} N}{2}\left[1 - \frac{\sin^2\left(\frac{\theta_{\max}}{2}\right)}{\left(\frac{\theta_{\max}}{2}\right)^2}\right] = \frac{\sigma_{cc}}{2}\frac{\beta 4\pi R_s^2}{A_{cc}}\left[1 - \frac{\sin^2\left(\frac{\theta_{\max}}{2}\right)}{\left(\frac{\theta_{\max}}{2}\right)^2}\right] \quad (3)$$

Where, for LAGEOS, $\theta_{max} = 43^o$ is the maximum acceptance angle of the solid cube corner, σ_{cc} = 2.834 x 10^6 m^2 [1] is the optical cross-section of a single cube corner at normal incidence, N = 426 is the total number retroreflectors on the spherical satellite, A_{cc} is the surface area occupied by a cube corner of diameter 38 mm, R_s = 29.8 cm is the satellite radius, and β = 0.435 is the "packing density". In computing the cross-section, Eq. (3) accounts for geometrical effects but not velocity aberration and therefore yields a peak value of 2.8x 10^7 m^2(in good agreement with NASA's RETRO computer program) whereas the average cross-section is about 7x$10^6$$m^2$ [1]. Using Eq. (2), θ_{max} can be expressed as a function of the time spread Δt and the satellite radius R_s, i.e.

$$\theta_{\max} = \sqrt{\frac{c\Delta t}{R_s\left[1 - \frac{nL(1+1/n^2)}{R_s}\right]}} \cong \sqrt{\frac{c\Delta t}{R_s}} \quad (4)$$

where the final approximation is valid in the large radius limit (R_s >> nL).

Figure 3 plots the peak satellite cross-section as a function of satellite radius and zero-to-zero pulse spreading for two values of the packing density β= 0.435 (LAGEOS) and 1 (ideal).

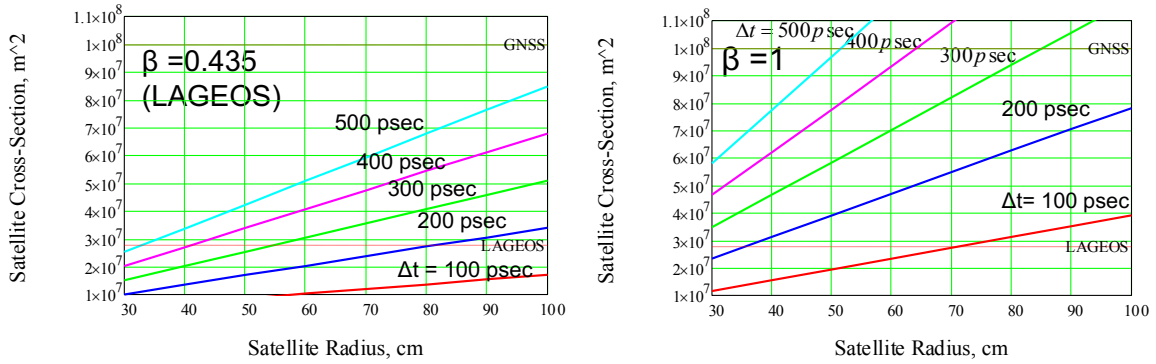

Figure 3: (a) Satellite cross-section as a function of satellite radius (R_s) and zero-to-zero pulse spreading (Δt) for a LAGEOS packing density of 38 mm diameter retros of β= 0.435; (b) same plot for an ideal (but unrealistic) packing density of β= 1. The peak cross-sections of LAGEOS and GNSS satellites appear as horizontal dashed red lines at 2.8x$10^7$$m^2$ and 1x$10^8$$m^2$ respectively.

3. GNSS AND GEOSTATIONARY SATELLITES

3.1 Replacing GNSS Flat Panels with a Segment of a Sphere

If we replace the current flat panels on GNSS satellites with a segment of a sphere with radius R_s, the minimum radius of the array footprint on the nadir-viewing side of the satellite, R_A, would be given by

$$R_A = R_S \tan(\theta_{\max} + \theta_{\lim}) \tag{5}$$

Substituting Eq. (4) for θ_{max} in Eq. (3) and setting $\sigma = 1x10^8$ m^2, the recommended cross-section for GNSS satellites, $\beta \sim 0.8$, $\theta_{lim} = 13.1^o$ and populating the satellite with commonly used 38 mm diameter retroreflectors, we can plot the radius of the spherical shell, R_S, and the radius of the footprint, R_A, as a function of the desired pulse spread in Figure 4a and the corresponding value of θ_{max} in Figure 4b. The value $\beta \sim 0.8$ is a compromise packing density which allows more retroreflectors per unit area on the spherical surface while still allowing "clocking" of the retroreflectors to at least partially correct for non-uniformities in the array cross-section due to the splitting of far field pattern of a single cube into six lobes to compensate for velocity aberration effects as in Figure 5.

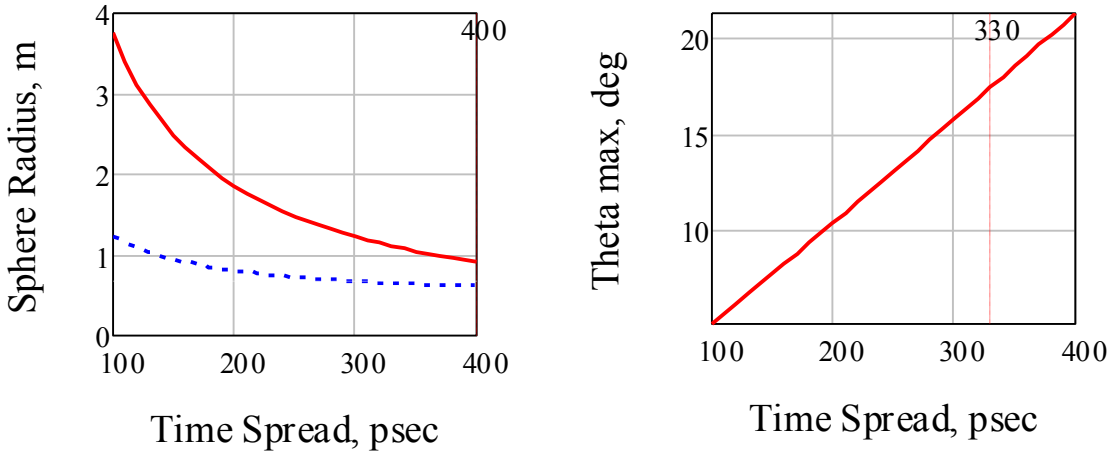

Figure 4: (a) Radius of the spherical segment housing standard 38 mm diameter retroreflectors (red line) and the radius of the segment footprint on the nadir side of the aircraft as a function of the pulse spreading ; (b) the value of θ_{max} as function of array time spread.

3.2 GNSS Retroreflector Size

As can be seen from Figure 4a, reduced array pulse spreading requires larger sphere segments and therefore larger footprints taking up valuable space on the nadir-viewing side of the spacecraft. To reduce target size, one can attempt to achieve still larger packing densities and/or increase the diameter of the retroreflector. From Eq. (3), we see that the array cross-section is proportional to

$$\frac{\sigma_{cc}\beta}{A_{cc}} \propto \beta A_{cc} \propto \beta D_{cc}^2 \tag{6}$$

since the cube cross-section, σ_{cc}, is proportional to A_{cc}^2. As seen in Figure 6, unlike LAGEOS, GNSS satellites have a very narrow range of velocity aberration centered at 26 μrad (top left). To implement this correction, each of the three dihedral angles in the cube must be spoiled by δ = 5.47 μrad (bottom left). This produces 6 lobes (bottom right) , one for each sector of the hexagonal cube (top right). The angular circumference passing through the center of the six lobes is equal to C=2πγ=163 μrad. By comparison, the 6 lobes of a single retro cover only 6 δ /C= 20% of that circumference. Thus, at least 6 clocking angles (0, 10, 20, 30, 40, 50 deg) are required to ensure that there is sufficient overlap between lobes created by adjacent retros to yield a more uniform cross-section response. A cursory analysis suggests that retro diameters up to 64 mm can be used, yielding the plots in Figure 7 for a fill factor of β =0.8.

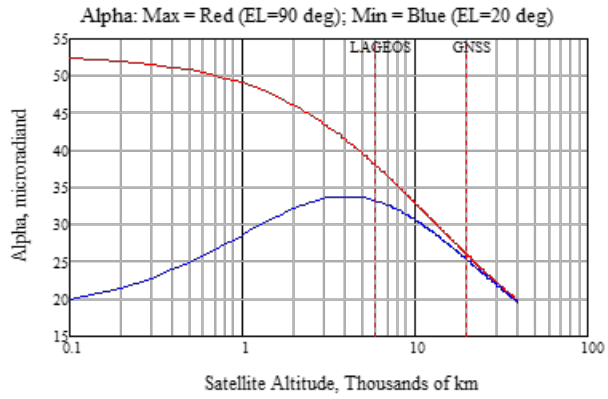

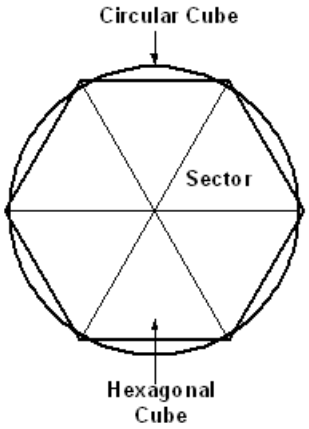

$$\gamma = \frac{4}{3}\sqrt{6}n\delta = 26\mu rad$$

$$\delta = \frac{3(26\mu rad)}{4\sqrt{6}(1.455)} = 5.47\mu rad$$

$$C = 2\pi\gamma = 163\mu rad$$

$$N_c = \frac{C}{6\delta} = \frac{163}{6(5.47)} = 5$$

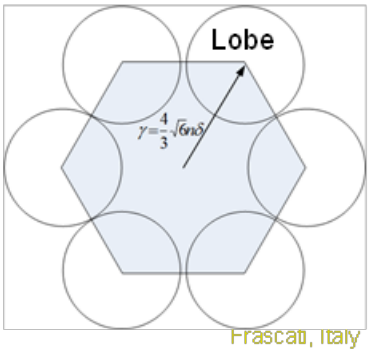

Figure 6: Clockwise TL to BL, TL: Velocity aberration range vs satellite altitude; TR: hexagonal corner cube face showing the 6 sectors; BR: separation of the retro far field pattern into six equal lobes by the dihedral offsets; BL: Equations giving the angular distance of the lobe center from the cube normal, the dihedral offset and approximate angular diameter of the lobe, the angular circumference of the circle passing through the lobes, and the minimum number of clocking positions required to fill in the angular gaps between the lobes.

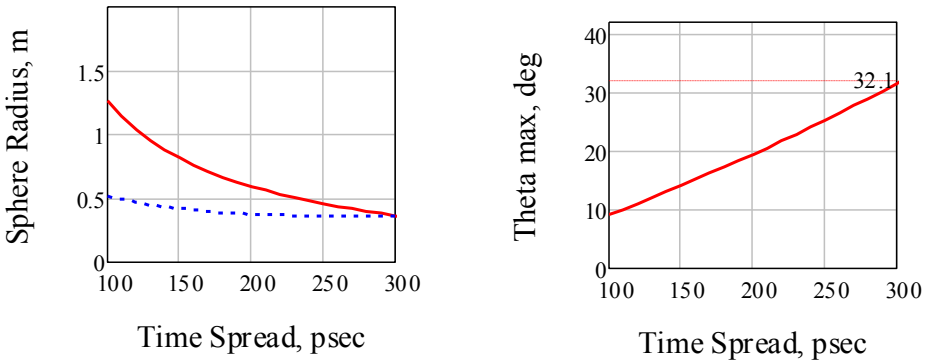

Figure7: Reduced array size assuming 64 mm diameter cubes and a fill factor of β=0.8

4. SUMMARY

For mm Accuracy LEO to MEO Geodetic Satellites:

- Design larger radius satellites to better match the incoming plane wave and increase the satellite weight to counteract increased satellite drag effects
- Reduce the range of accepted incidence angles through the use of hollow retros or recessed hollow or solid retros to further reduce the satellite impulse response. A further advantage is that incidence angles with $\theta_{max} < 17^{o}$ do not leak light in solid TIR reflectors.
- Maximize the packing density of retros to achieve the necessary optical cross-section in the smallest diameter satellite.
- Selecting cube diameters, spoiling, and clocking to best match the "α annulus" while favoring high zenith (low elevation) observing angles is key to efficient array design.

For GNSS and GEO Satellites:

- Replace current flat panels with segments of large, densely packed spheres, at the expense of a larger footprint on the nadir mounting surface, in order to present a uniform and much narrower impulse response over the full range of interrogation angles
- Range accuracy and signal uniformity would benefit from using a segment of a large sphere

REFERENCES

[1] J. Degnan, Millimeter Accuracy Satellite Laser Ranging: A Review, in Contributions of Space Geodesy to Geodynamics: Technology, D. E. Smith and D. L. Turcotte (Eds.), AGU Geodynamics Series, Volume 25, pp. 133-162, 1993.

[2] J. Degnan, R. Machan, A Proposed Multifunctional Multichannel Receiver for SGSLR, 19th International Workshop on Laser Ranging, Annapolis, MD USA, October, 2014

[3] J. Degnan, The Effects of Threshold and Signal Strength on LAGEOS Normal Point Biases 9th International Workshop on Laser Ranging, Canberra, Australia, November, 1994.